Galilean and Relativistic Nonlinear Wave equations: an Hydrodynamical Tool?

Malek ABID[1], *Marc BRACHET*[2], *Fabrice DEBBASCH*[3] *and Caroline NORE*[2]

[1] Institut de Recherche sur les Phénomènes Hors Equilibre.
UMR CNRS et Université d'Aix-Marseille I, service 252, Centre St-Jérôme,
13397 Marseille Cedex 20, France
[2] Laboratoire de Physique Statistique
CNRS URA 1306, ENS Ulm
24 Rue Lhomond, 75231 Paris Cedex 05, France
[3] Laboratoire de Radioastronomie
ENS Ulm, 24 Rue Lhomond, 75231 Paris Cedex 05, France
Observatoire de Paris
Section de Meudon, place J.-Jansen
F-92195 Meudon Cedex, France

The connexion of nonlinear wave equations with the dynamics of barotropic fluids by Madelung's transformation is reviewed in the case of fluids with arbitrary equations of state. Numerical simulations of the Nonlinear Schrődinger Equation (NLSE) reproducing the instabilities of non rotating and rotating cylindrical jets are presented. It is shown that NLSE, a dynamical model of superflows, reproduces many flow features usually obtained in the context of Euler or Navier-Stokes equations.

A generalization to relativistic wave equations and superfluids is reviewed. The Galilean limit is shown to be NLSE. A model for a relativistic self-gravitating superfluid is obtained by minimally coupling the wave equation to Einstein's gravity. Applications corresponding to static stars and isotropic cosmologies are discussed.

1 Introduction

It has been known for some time that Madelung's transformation maps the (defocusing) Nonlinear Schrődinger Equation (NLSE) into hydrodynamical equations for a compressible fluid with dispersion. In the early 80's [1], E. Spiegel emphasized that the dynamics of irrotational barotropic fluids, with arbitrary equations of state, can be linked to NLSE-type equations with suitable nonlinearities. Furthermore NLSE contains topological defects that are known to follow Eulerian dynamics in the incompressible limit [2, 3, 4]. These topological defects correspond to the quantum vortices of superfluid Helium [5]. In this context, NLSE is the correct dynamical equation of motion for superfluids [6].

More recently [7, 8, 9, 10, 11], numerical simulations of NLSE have been used to probe its ability to reproduce typical fluid dynamical phenomena. One of the motivations behind this recent surge of interest is the possibility of understanding the details of intricate dynamical mechanisms, such as vortex nucleation [7] and vortex-sound interaction [12], in superfluid Helium.

E. Tirapegui and W. Zeller (eds.), Instabilities and Nonequilibrium Structures V, 33–52.

A special relativistic generalization of the NLSE dynamics, using the nonlinear Klein Gordon equation (NLKGE), has been studied by J.C. Neu [3, 13] with emphasis on the derivation of equations of motion for vortices, without taking into account the acoustic sector of the dynamics. In a general relativistic framework, static solutions of this wave equation describing boson stars have already been considered by various authors [14, 15], but without a Madelung-like correspondence to usual hydrodynamics. Such a correspondence was recently given in [16].

The purpose of this paper is to synthesize some of the recently obtained results. It is organized as follows. Section 2 is devoted to the fluid dynamical representation of NLSE. Numerical simulations of NLSE in the context of free-shear flows instabilities are presented in section 3. Section 4 concerns the special relativistic generalization of the material presented in section 2. Section 5 contains applications to general relativistic self-gravitating fluids. And section 6 is our conclusion.

2 Fluid dynamical representation of NLSE

In this section, we present the hydrodynamical form of NLSE with an arbitrary nonlinearity, corresponding to a barotropic fluid with an arbitrary equation of state. Basic hydrodynamical features such that acoustic propagation and time independent solutions are also discussed.

2.1 Formal correspondence

Perhaps the most direct way to understand the scope and generality of the connexion between nonlinear waves and fluid dynamics is to consider the following action [1] :

$$\mathcal{A} = 2\alpha \int dt \left\{ d^3x \left(\frac{i}{2} \left(\overline{\psi} \frac{\partial \psi}{\partial t} - \psi \frac{\partial \overline{\psi}}{\partial t} \right) \right) - \mathcal{F} \right\} \tag{1}$$

with

$$\mathcal{F} = \int d^3x \left(\alpha |\nabla \psi|^2 + f(|\psi|^2) \right) \tag{2}$$

where $\psi(\boldsymbol{x}, t)$ is a complex wave field and $\overline{\psi}$ its complex conjugate, α is a positive real constant and f is a polynomial in $|\psi|^2 \equiv \overline{\psi}\psi$ with real coefficients :

$$f(|\psi|^2) = -\Omega|\psi|^2 + \frac{\beta}{2}|\psi|^4 + f_3|\psi|^6 + \ldots + f_n|\psi|^{2n} \tag{3}$$

The NLSE is the Euler-Lagrange equation of motion for ψ corresponding to (1), it reads

$$\frac{\partial \psi}{\partial t} = -i \frac{\delta \mathcal{F}}{\delta \overline{\psi}},$$

or

$$\frac{\partial \psi}{\partial t} = i(\alpha \nabla^2 \psi - \psi f'(|\psi|^2)) \tag{4}$$

Madelung's transformation [5, 1]

$$\psi = \sqrt{\rho} \exp\left(i\frac{\varphi}{2\alpha}\right) \tag{5}$$

maps the nonlinear wave dynamics of ψ into equations of motion for a fluid of density ρ and velocity $\boldsymbol{v} = \nabla\varphi$. Indeed with the help of (5), (1) can be written

$$\mathcal{A} = -\int dt d^3x \left(\rho\frac{\partial\varphi}{\partial t} + \frac{1}{2}\rho(\nabla\varphi)^2 + 2\alpha f(\rho) + \frac{1}{2}(2\alpha\nabla(\sqrt{\rho}))^2\right) \tag{6}$$

and the corresponding Euler-Lagrange equations of motion read

$$\frac{\partial\rho}{\partial t} + \nabla\cdot(\rho\boldsymbol{v}) = 0 \tag{7}$$

$$\frac{\partial\varphi}{\partial t} + \frac{1}{2}(\nabla\varphi)^2 + 2\alpha f'(\rho) - 2\alpha^2\frac{\Delta\sqrt{\rho}}{\sqrt{\rho}} = 0 \tag{8}$$

Without the last term of (8) (the so-called "quantum pressure" term), these equations are the continuity and Bernoulli equations [17] for an isentropic, compressible, irrotational fluid.

It is possible to use this identification to define the corresponding "thermodynamical functions". Being isentropic, the fluid is barotropic, and there is thus only one independent thermodynamical variable. The Bernoulli equation readily gives the fluid's enthalpy *per unit mass* as

$$h = 2\alpha f'(\rho). \tag{9}$$

On the other hand, the $\frac{1}{2}\rho(\nabla\varphi)^2$ term of (6) is seen to correspond to kinetic energy. Thus the fluid's internal energy *per unit mass* is given by

$$e = \frac{2\alpha f(\rho)}{\rho}. \tag{10}$$

The general thermodynamical identity

$$h = e + p/\rho, \tag{11}$$

gives the fluid's pressure

$$p = 2\alpha(\rho f'(\rho) - f(\rho)). \tag{12}$$

The physical dimensions of the variables used in (2) and (3) are fixed by the following considerations. Madelung's transformation (5) imposes that $[|\psi|^2] = [\rho] = M\,L^{-3}$ and $[\alpha] = L^2\,T^{-1}$. Using (10), one gets $[f(\rho)/\rho] = T^{-1}$ and thus, from (3), $[\Omega] = T^{-1}$, $[\beta] = T^{-1}\,\rho^{-1}$ and $[f_i] = T^{-1}\,\rho^{1-i}$. Note that, in the case of a Bose condensate of particles of mass m, α has the value $\hbar/2m$ [6].

2.2 Acoustic regime

Dispersion relation The nature of the extra quantum pressure term in (8) is best understood by looking at the dispersion relation corresponding to acoustic waves propagating around a constant density level ρ_0. Setting $\rho = \rho_0 + \delta\rho$ (with $f'(\rho_0) = 0$), $\nabla\varphi = \delta u$ in (7) and in the gradient of (8), one gets (keeping only the linear terms) :

$$\partial_t \delta\rho + \rho_0 \nabla \delta u = 0$$
$$\partial_t \delta u + 2\alpha f''(\rho_0)\nabla\delta\rho - 2\alpha^2 \Delta \frac{\nabla\delta\rho}{2\rho_0} = 0$$

or

$$\partial_t{}^2 \delta\rho = 2\alpha\rho_0 f''(\rho_0)\Delta\delta\rho - \alpha^2\Delta^2\delta\rho.$$

The dispersion relation for an acoustic wave $\delta\rho = \epsilon(\exp(i(\omega t - \boldsymbol{k}\cdot\boldsymbol{x})) + c.c.)$ (with $\epsilon \ll 1$) is thus

$$\omega = \sqrt{2\alpha\rho_0 f''(\rho_0)\boldsymbol{k}^2 + \alpha^2\boldsymbol{k}^4} \tag{13}$$

This relation shows that the quantum pressure has a dispersive effect that becomes important for large wave numbers. For small wavenumbers, one recovers the usual propagation, with a sound velocity given by

$$c = \left(\frac{\partial p}{\partial \rho}\right)^{\frac{1}{2}} = \sqrt{2\alpha\rho_0 f''(\rho_0)}.$$

The length scale $\xi = \sqrt{\alpha/(\rho_0 f''(\rho_0))}$ at which dispersion becomes noticeable is known as the "coherence length".

Note that, in the context of superfluid helium modelling, it has been suggested [18] to replace (2) by a non local term of the form

$$\mathcal{F}_{nl} = \int d^3x\alpha|\nabla\psi|^2 + \int d^3x_1 d^3x_2 \frac{1}{2}|\psi|^2(\boldsymbol{x_1})V(|\boldsymbol{x_1} - \boldsymbol{x_2}|)|\psi|^2(\boldsymbol{x_2}).$$

It is easy to check that with such a term, one gets the following dispersion relation

$$\omega = \sqrt{2\alpha\rho_0\hat{V}(\boldsymbol{k})\boldsymbol{k}^2 + \alpha^2\boldsymbol{k}^4}$$

where $\hat{V}(\boldsymbol{k})$ is the fourier transform

$$\hat{V}(\boldsymbol{k}) = \int d^3x e^{i\boldsymbol{k}\cdot\boldsymbol{x}}\, V(|\boldsymbol{x}|).$$

The function V can then be chosen such that the dispersion relation fits the one experimentally known for helium. Let us remark here that the same goal can be achieved in a local framework by Taylor expanding the function $\hat{V}(\boldsymbol{k})$. This amounts to add to (2) dispersive terms of the form :

$$\mathcal{F}_d = \int d^3x|\psi|^2 g(\Delta)|\psi|^2,$$

where $g(\Delta)$ is a polynomial in the laplacian operator. We shall not consider such dispersive terms in the rest of this paper.

Nonlinear acoustics The description given by linear acoustic can be somewhat improved by including the dominant nonlinear effects. Such an equation was derived in [9].

Numerical simulations of NLSE in one space dimension using a standard Fourier pseudo-spectral method [19] can be used to study the acoustic regime triggered by an initial disturbance of the form :

$$\psi(x) = 1 + ae^{-\frac{x^2}{l^2}}.$$

A simulation result is displayed in Figures 1. The nonlinear effect present in these Figs can be distinguished from a purely linear dispersive effect by the scale of the generated wave-trains. In the nonlinear case, the scale of the wave-train is much smaller than the scale of the initial perturbation. The pulses travel at supersonic speed. The propagation speed can be explained [9] as a nonlinear renormalization of sound velocity.

The data presented in Figs 1 also show that the shocks that would have appeared under compressible Euler dynamics (i.e. following Eq. (8) without the last term in r.h.s.) have been regularized by the dispersion. There is no evidence of finite-time singularity in our numerics. The spectrum of the solution (data not shown) is well resolved, with a conspicuous exponential tail.

2.3 Time independent solutions

Further insight on the connexion between wave and fluid dynamics can be obtained by considering stationary solutions of the equations of motion. Indeed, by inspection of (1), time independent solutions of NLSE (4), are also solutions of the Real Ginzburg-Landau Equation (RGLE)

$$\frac{\partial \psi}{\partial t} = -\frac{\delta \mathcal{F}}{\delta \overline{\psi}} = (\alpha \nabla^2 \psi - \psi f'(|\psi|^2)). \tag{14}$$

They are thus extrema of the free energy $\mathcal{F}$.

The simplest solution of this type corresponds to a constant density fluid at rest. In this simple case, ψ is constant in space and (14) reads

$$f'(|\psi|^2) = -\Omega + \beta|\psi|^2 + 3f_3|\psi|^4 + \ldots + nf_n|\psi|^{2n-2} = 0. \tag{15}$$

This equation, for given values of the coefficients β and $f_i, i = 3, \ldots, n$ relates the fluid density $|\psi|^2$ to the value of Ω. Note that the Ω term of f does not play a crucial role in the NLSE dynamics. Indeed, it could be removed from the Bernoulli equation (8) by the change of variable $\varphi \rightarrow \varphi + 2\alpha\Omega t$ that amounts to a change of phase $\psi \rightarrow \psi e^{i\Omega t}$ in NLSE (4). We will however, by convention, not perform these changes of variable, in order that stationary solutions of (14) coincide with stationary solutions of (4). The Ω term of f will thus be fixed by the fluid's density through (15).

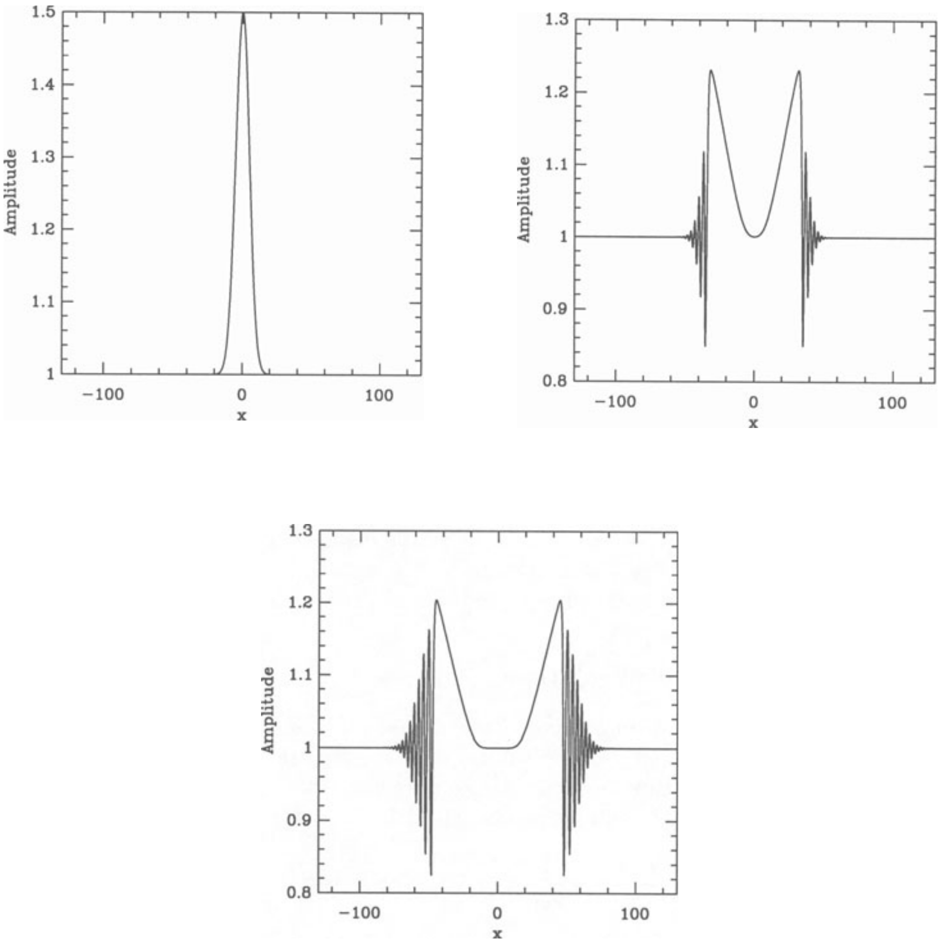

Fig. 1. Numerical integration of NLSE in 1D with an initial perturbation of amplitude ($a = 0.5$) and large width ($l = 10\ \xi$): (a) amplitude of the initial data. (b) amplitude of the solution at $t = 20$. (c) amplitude of the solution at $t = 30$.

Note that scales significantly smaller than the length scale on the initial data have been generated through nonlinear effects.

Another important type of time-independent solutions of NLSE are the vortex solutions. Madelung's transformation is singular when $\rho = 0$ (i.e. when both $\Re(\psi) = 0$ and $\Im(\psi) = 0$, see Figure 2 (a)). As two conditions are required, the singularities generically happen on points in two dimensions and lines in three dimensions. The circulation of $\boldsymbol{v}$ around such a generic singularity is $\pm 4\pi\alpha$. These topological defects are known in the context of superfluidity as "quantum vortices" [5]. Solutions of (14) with cylindrical symmetry can be obtained numerically [20]. The profile of a vortex is shown on Figure 2 (b). The density admits a horizontal asymptote near the core (see Figure 3 (c)) while the velocity diverges as the inverse of the core distance (see Figure 3 (d)). Then the momentum density $\rho\boldsymbol{v}$ is a regular quantity shown on Figure 4 (f).

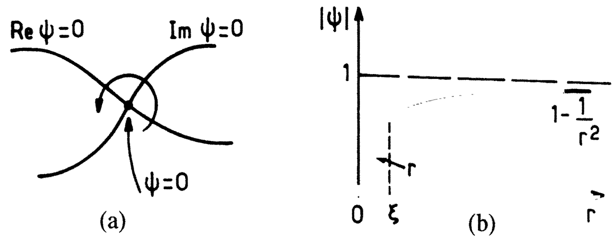

Fig. 2. Nodal point of the condensate wave function and vortex profile.

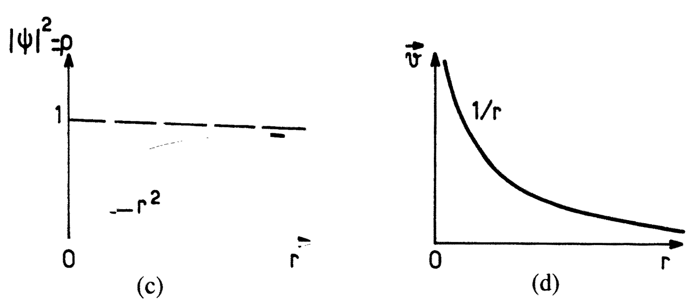

Fig. 3. Vortex density and velocity profile.

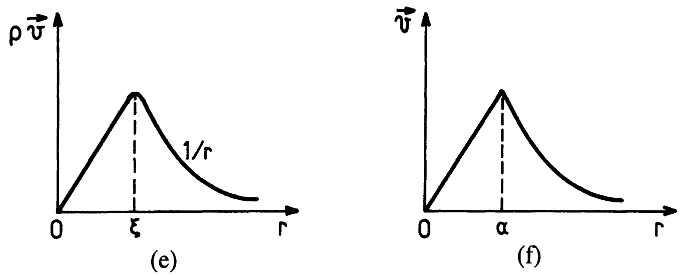

Fig. 4. Quantum vortex momentum versus classical vortex momentum (vorticity patch of radius a).

3 Numerical study of vortex dynamics

Under compressible fluid dynamics, an arbitrary chosen initial condition will generally lead to a regime dominated by acoustic radiation. In order to study vortex dynamics using NLSE, we thus need to prepare the initial data in such a way that the acoustic emission is as small as possible.

3.1 Preparation method

We know that the RGLE (14) starting with an initial data containing a nodal line converges towards the exact time independent vortex solution ψ_v described at the end of section (2.3).

The ARGLE procedure The procedure we have developed is a generalization of this property of RGLE. Our aim is to prepare an arbitrary assembly of moving vortices. To do so, we use the (active) Galilean invariance of NLSE that maps any solution of NLSE $\psi(\boldsymbol{x},t)$ into another solution of NLSE whose associated velocity and density fields are Galilean transforms of those associated to ψ. The Galilean transformation of NLSE reads:

$$\psi(\boldsymbol{x},t) \to \psi(\boldsymbol{x}-\boldsymbol{u}t,t)\ \exp\left(i\left(\frac{\boldsymbol{u}}{2\alpha}\cdot\boldsymbol{x}-\frac{u^2}{4\alpha}t\right)\right),$$

($\boldsymbol{u}$ being the constant velocity of the boost). Thus, the initial solution $\tilde{\psi}(\boldsymbol{x}) = \psi_v(\boldsymbol{x})\exp(i\frac{\boldsymbol{u}}{2\alpha}\cdot\boldsymbol{x})$ corresponds to a vortex translating with velocity $\boldsymbol{u}$. It can be directly obtained as a stationary solution of the following equation

$$\frac{\partial\psi}{\partial t} = \alpha\nabla^2\psi - \psi f'(|\psi|^2) - i\boldsymbol{u}\cdot\nabla\psi - \frac{u^2}{4\alpha}\psi \qquad (16)$$

that we will call the Advective Real Ginzburg-Landau Equation (ARGLE). This equation corresponds to an extremum of the following modified free energy:

$$\mathcal{F} = \int d^3\boldsymbol{x} \left(\alpha|\nabla\psi - i\frac{\boldsymbol{u}}{2\alpha}\psi|^2 + f(|\psi|^2)\right). \tag{17}$$

Our preparation method consists in using (16) and (17) with a given *space dependent* divergence less velocity field $\boldsymbol{u}(\boldsymbol{x})$. Using the Madelung transformation, (17) reads :

$$\mathcal{F} = \frac{1}{2\alpha}\int d^3\boldsymbol{x} \left(\frac{1}{2}(2\alpha\nabla\sqrt{\rho})^2 + 2\alpha f(\rho) + \frac{1}{2}\rho(\nabla\varphi - \boldsymbol{u}(\boldsymbol{x}))^2\right).$$

The last term in the r.h.s will be minimum if the potential velocity $\nabla\varphi$ is as close as possible to the imposed advective velocity $\boldsymbol{u}(\boldsymbol{x})$.

Initial conditions for ARGLE For a constant $\boldsymbol{u}$, the absolute minimum of $\mathcal{F}$ is given by $\psi = \sqrt{\Omega/\beta}\exp(i\boldsymbol{u}\cdot\boldsymbol{x}/(2\alpha))$ which corresponds to a fluid moving with the imposed velocity $\boldsymbol{u}$. Another stationary solution of ARGLE is $\psi_0 = \sqrt{\Omega/\beta}\left(1-(u^2/4\alpha\Omega)\right)^{1/2}$ which corresponds to a fluid with zero velocity. The linear stability study of ψ_0 can be obtained in term of normal modes using $\psi = \psi_0(1 + u_0\exp(\sigma t + ikx) + v_0\exp(\sigma t - ikx))$. We find :

$$\sigma = -\Omega\left(1 - \frac{u^2}{4\alpha\Omega}\right) - \alpha k^2 \pm \sqrt{u^2k^2 + \Omega^2\left(1 - \frac{u^2}{4\alpha\Omega}\right)^2}, \tag{18}$$

Note that this stability computation is formally identical to the one leading to the Eckhaus instability of convective rolls [21]. Therefore, in the stable Eckhaus region ($u/c = u/(\sqrt{2\alpha\Omega(1-(u^2/4\alpha\Omega))}) < 1$), the stationary solution ψ_0 corresponds to a local minimum of $\mathcal{F}$. In general, with a variable $\boldsymbol{u}(\boldsymbol{x})$, we also expect several branches of stable solutions for (16) corresponding to local minima of $\mathcal{F}$.

3.2 Numerical results for 3D free-shear flows

To carry out the numerical integration, we use standard pseudo-spectral codes [19]. In the lateral directions, we use sine-cosine transforms to implement free-slip boundary conditions away from the flow's center. Our codes were validated by cross-checking with general periodic codes and linear theory [10].

Round jet The jet's profile is that studied by [22] :

$$u(r) = (U_0/2)[1 + \tanh(R(1 - r/R)/(2\theta))],$$

where U_0 is the centerline velocity on the x jet's axis, $r = \sqrt{y^2+z^2}$ is the radial coordinate, θ is the momentum thickness and R is the jet radius. The initial data for ARGLE, ψ_0, is obtained by interpolating between a fluid moving with the velocity U_0 at the center of the jet to a motionless fluid far from the jet :

$$\psi_0 = \sqrt{\frac{\Omega}{\beta}} \left[\frac{1}{2} \left(1 - th \left(\frac{r-R}{\theta} \right) \right) \exp \left(i \frac{U_0 x}{2\alpha} \right) + \frac{1}{2} \left(1 + th \left(\frac{r-R}{\theta} \right) \right) \right] \quad (19)$$

The ARGLE converged solution consists in a periodic array of vortex rings of radius R, separated by a length $l = 4\pi\alpha/U_0$. Under NLSE dynamics, this ARGLE converged solution yields a moving periodic array of vortex rings, with little acoustic emission. Adding a small non-axisymmetric perturbation, we obtain a behavior similar to that experimentally observed by Kambe[23] (see Figs 5). The motion of each azimuthally perturbed vortex ring is a rigid rotation in the direction opposite to that of peripheral fluid rotation around the filament.

Swirling jet We have also studied a swirling jet [24] :

$$\begin{aligned} u(r) &= U_0 \exp(-(r/R)^2), \\ v(r) &= -\frac{z\,R}{r^2}\, q\, (1 - \exp(-(r/R)^2)), \\ w(r) &= \frac{y\,R}{r^2}\, q\, (1 - \exp(-(r/R)^2)), \end{aligned}$$

where q is the rotation rate. The initial data for ARGLE, ψ_0, is obtained by multiplying a scalar field corresponding to the jet, as described above (19), with a field containing as many axial defect filaments as there are quantized quanta $4\pi\alpha$ in the global circulation $2\pi q R$.

The ARGLE converged solution consists in locked-up helices. Under NLSE dynamics, the helices undergo a cork-screw like motion, with little acoustic emission. The dynamics corresponding to an helix with a (small) random perturbation is rich and complex and includes reconnection phenomena (see Figs 6). These reconnection events and the corresponding rapid spreading of the rotating jet can be related to vortex breakdown observed in turbulent flows [25].

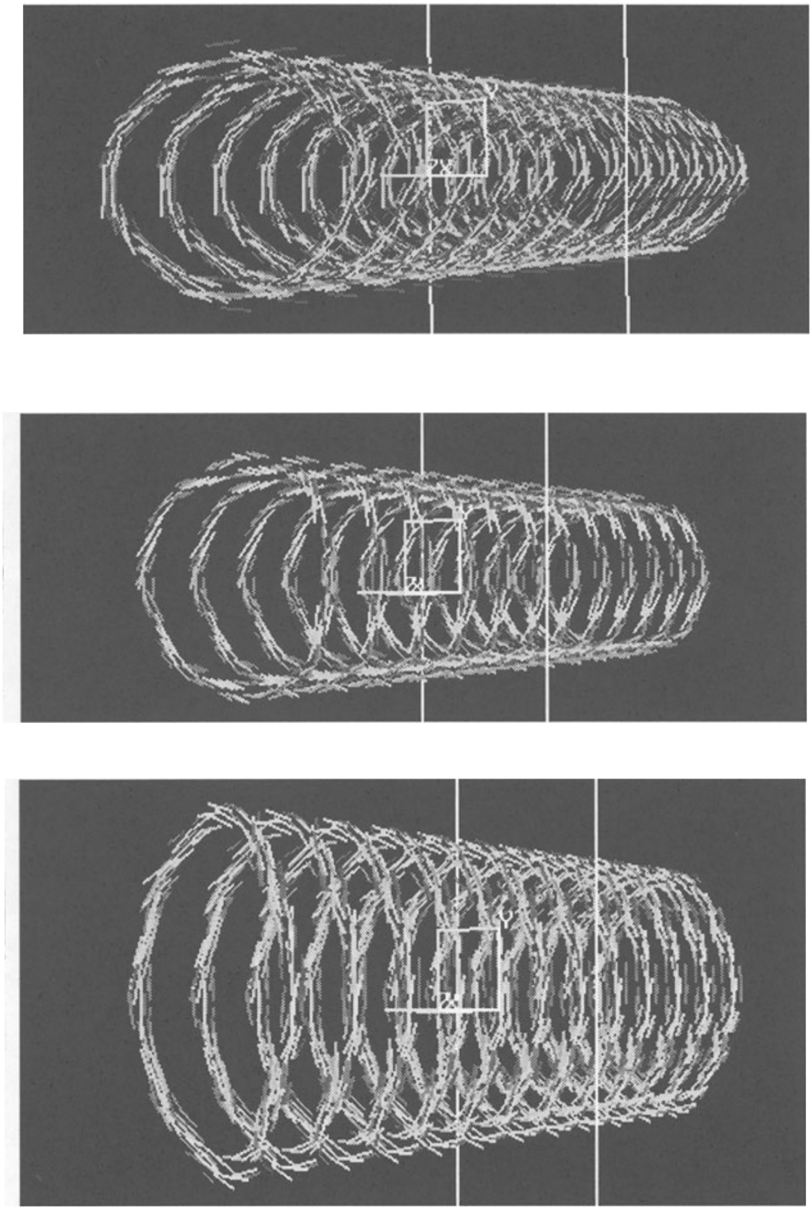

Fig. 5. Azimuthal perturbation of the jet ($m = 2$ azimuthal wave number) : slantwise views at different times (the phenomenon is time-periodical). The jet parameters are : $U_0 = 1$, $\theta = 0.16$ and $R = 1$ with a vortex core size $\xi = 0.07$.

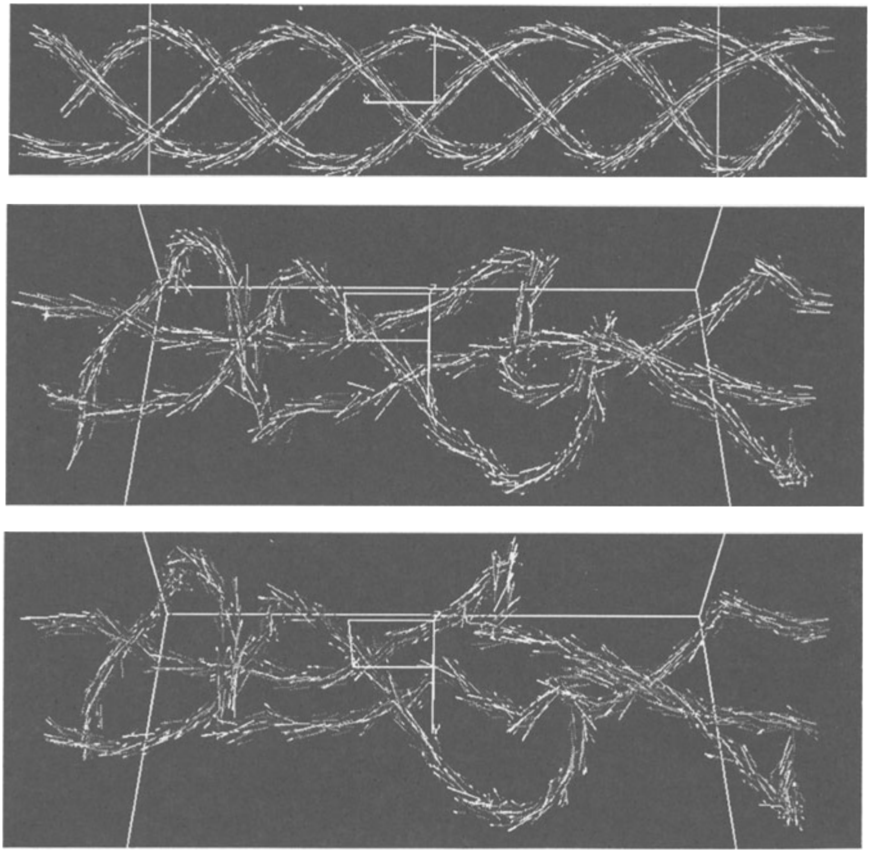

Fig. 6. Swirling jet flow : a) slantwise view of the initial data for the NLSE, b) Reconnection event : before, d) after the reconnection. The jet parameters are the same as in Figure 5 with $q = 0.8$ and $\xi = 0.047$. The amplitude of the random perturbation is 0.1.

4 Fluid dynamical representation of NLKGE in flat space-time

This section contains the special relativistic generalization of the material presented in section 2.

Notations: Throughout the two last sections, the space-time coordinates will be written $x^\mu = (ct, \boldsymbol{x})$, corresponding to the Minkovskian metric given by $diag(1, -1, -1, -1)$.

4.1 Formal correspondence

Let us now consider the following action [16, 26]:

$$\mathcal{A}_r = \frac{1}{c}\int d^4x L$$

$$L = 2\alpha^2 \Phi_\nu \Phi^{\nu *} - 2\alpha f(|\Phi|^2) - \frac{c^2}{2}|\Phi|^2 \tag{20}$$

where Φ is a complex scalar field and α and f have already been defined in section (2.1). Extremizing $\mathcal{A}_r$ with respect to Φ^*, we obtain the NLKGE:

$$2\alpha^2 \Phi_\mu^{\ \mu} + 2\alpha \Phi f'(|\Phi|^2) + \frac{c^2}{2}\Phi = 0 \tag{21}$$

Equations (20) and (21) are the special relativistic generalizations of (1) and (4). As a matter of fact, if one introduces a new field ψ by the relation:

$$\psi = \Phi \exp\left(i\,\frac{c^2}{2\alpha}\,t\right) \tag{22}$$

Equations (20) and (21) give back (1) and (4) (for ψ) if one lets c tend to infinity.

As in the Galilean case, a formal correspondence between (21) and special relativistic potential flows of barotropic fluids can be achieved by using the Madelung transform:

$$\Phi = \sqrt{\rho}\exp\left(i\,\frac{\sigma}{2\alpha}\right) \tag{23}$$

If one defines [16] the velocity of the fluid u, the scalar particle density n and the enthalpy density w by

$$u_\mu = -\frac{\sigma_\mu}{(\sigma_\mu \sigma^\mu)^{1/2}} \tag{24}$$

$$n = \frac{\rho}{mc}(\sigma_\mu \sigma^\mu)^{1/2} \tag{25}$$

$$w = \rho(\sigma_\mu \sigma^\mu) \tag{26}$$

the conserved current j associated to the phase invariance of $\mathcal{A}_r$ takes, after a convenient normalization, the usual hydrodynamical form:

$$j_\mu = n\, u_\mu \tag{27}$$

and one also obtains from (24), (25), (26) the normal special relativistic condition for potential flows:

$$mc\sigma_\mu = -\frac{w}{n}u_\mu \tag{28}$$

It should be noted at this point that, for the preceding identifications to be meaningful, the current j has to be time-like in the space-time region under consideration. This is in particular the case if the relativistic effect only constitutes corrections to the main Galilean phenomena. This point is further discussed in [16].

The equation of motion (21) delivers the following relations between n, w and ρ, separating real and imaginary parts:

$$n = \frac{\sqrt{\rho}}{mc}\left(\rho c^2 + 4\alpha\rho f'(\rho) + 4\alpha^2\sqrt{\rho}\,(\sqrt{\rho})_\mu^\mu\right)^{1/2} \tag{29}$$

$$w = \rho c^2 + 4\alpha\rho f'(\rho) + 4\alpha^2\sqrt{\rho}\,(\sqrt{\rho})_\mu^\mu \tag{30}$$

so that the enthalpy per particle H reads

$$H = mc\left(c^2 + 4\alpha f'(\rho) + 4\alpha^2\frac{(\sqrt{\rho})_\mu^\mu}{\sqrt{\rho}}\right)^{1/2} \tag{31}$$

If quantum pressure terms were absent, *i.e.* for ordinary barotropic fluids, it would be possible to deduce automatically from (29), (30) and (31) the correct expression for the pressure p, using the standard thermodynamical relation (with vanishing entropy):

$$dp = n\,dH \tag{32}$$

This would give:

$$p = 2\alpha(\rho f'(\rho) - f(\rho)) \tag{33}$$

However, if the dispersive terms are taken into account, it is no longer possible to eliminate ρ from (29) and (30) to obtain the enthalpy density as a functional of the particle density and its derivatives. It is convenient to retain (33) as the definition of p and to further define the internal energy density ε by the usual relation:

$$\varepsilon = w - p \tag{34}$$

The definitions (29), (30), (31), (34) neglecting the dispersive quantum pressure term give valid thermodynamical relations. However we keep this dispersive term in order for (28) to hold exactly.

Let us now rapidly investigate how the correct Galilean thermodynamics can be recovered from the preceding results. The Galilean particle density is equivalent to n as c tends to infinity [16]. From (29), we therefore deduce that the Galilean particle density is represented by ρ/m. The Galilean counterpart of H is obtained for c tending to infinity. (31) gives immediately that:

$$H \sim mc^2 + 2\alpha m f'(\rho) - 2\alpha^2 m\frac{\Delta\sqrt{\rho}}{\sqrt{\rho}} \tag{35}$$

The first term represents a rest-mass energy, the third one is clearly a dispersive term, not usually included in the Galilean definition of thermodynamical quantities. Recalling that the thermodynamical enthalpy (31) is defined *per particle*, whereas the Galilean one (9) is defined *per unit mass*, the second term coincides with (9). Similarly, the Galilean equivalent of ε/n is:

$$\frac{\varepsilon}{n} \sim mc^2 + 2\alpha m \frac{f(\rho)}{\rho} - 2\alpha^2 m \frac{\Delta\sqrt{\rho}}{\sqrt{\rho}} \tag{36}$$

In the same way as for H, the second term, divided by m, coincides with the Galilean internal energy *per unit mass* (10). Finally, using the preceding results, (28) implies that, in the Galilean limit,

$$\boldsymbol{v} = \nabla\sigma = \nabla\varphi \tag{37}$$

as it should be. One can also investigate how the Galilean limiting procedure works on the stress-energy tensor as a whole. This has been done in [16] and we refer the reader to this article for further insights on the question.

4.2 Acoustic phenomena

Dispersion relation In section (2.2), acoustic phenomena were introduced to help in the understanding of the extra quantum pressure dispersive terms present in $\mathcal{A}$. The corresponding relativistic dispersion relation is obtained [16] by linearization of (21) around (22) with $f'(|\Phi_0|^2) = 0$. It reads

$$\left(\frac{\omega^2}{c^2} - \boldsymbol{k}^2\right)\left(\boldsymbol{k}^2 - \frac{\omega^2}{c^2} + \frac{2}{\alpha}|\Phi_0|^2 f''(|\Phi_0|^2)\right) + \left(\frac{\omega}{\alpha}\right)^2 = 0 \tag{38}$$

Letting c tend to infinity, one obtains (13).

Nonlinear acoustics If one takes as the definition of an acoustic wave that the corresponding density perturbation and 3-velocity are both small quantities of the same order, conventionally chosen to be the first, it can be easily shown [26] that there actually exist an infinity of different acoustic sectors, both for the NLKGE and the NLSE. Each sector is characterized by a real number η, $0 \leq \eta \leq 1$, such that the phase σ is of order η, and the 4D gradient, when acting on ρ and σ, is of order $1-\eta$. The scaling studied in section (2.2) corresponds to $\eta = 1$, and is the one most commonly worked with in hydrodynamical literature. However, that this is clearly not the only interesting one comes from the fact that the 1D NLKGE and NLSE admit soliton solutions which, in the acoustic regime, correspond to $\eta = 1/2$.

It turns out that it is possible, for all sectors for which $\eta \neq 1$, to obtain [26] a variational principle involving the single field σ, capable of delivering a non-linear equation for this field alone which completely describes the wave propagation at any desired perturbation order and the associated conserved quantities as well. We will not dwell into further details here.

4.3 Time-independent solutions

Let us now elaborate on the special relativistic generalization of the RGLE and on some particular 'static solutions' that can be found with its help. Since time is naturally not a Lorenz scalar, the concept of a static solution and the developments that follow presuppose the choice of a particular inertial frame *ab initio.*

The NLSE and the NLKGE can be put under a hamiltonian form which naturally simplifies the obtaining of the associated RGLE. Let $\mathcal{H}(p,q)$ be the Hamiltonian under consideration. The equations of motion generated by $\mathcal{H}$ take the well-known form:

$$\begin{aligned} \frac{\partial \mathcal{H}}{\partial p} &= \dot{q} \\ \frac{\partial \mathcal{H}}{\partial q} &= -\dot{p} \end{aligned} \tag{39}$$

and the corresponding RGLE simply read:

$$\begin{aligned} \frac{\partial \mathcal{H}}{\partial p} &= -\dot{p} \\ \frac{\partial \mathcal{H}}{\partial q} &= -\dot{q} \end{aligned} \tag{40}$$

Starting from the Lagrangian density L, considered as a function of $\delta = \rho^{1/2}$and σ:

$$L = -\delta^2 \sigma_t - \frac{\delta^2}{2} (\nabla \sigma)^2 + \frac{\delta^2}{2\, c^2} \sigma_t^2 - 2\alpha f(\delta^2) - 2\alpha^2 (\nabla \delta)^2 + \frac{2\alpha^2}{c^2} \delta_t^2 \tag{41}$$

one finds the following expression for the conjugate momenta (with respect to time) associated to these quantities:

$$\begin{aligned} \Pi_\delta &= \frac{4\alpha^2}{c^2} \delta_t \\ \Pi_\sigma &= \frac{\delta^2 \sigma_t}{c^2} - \delta^2 \end{aligned} \tag{42}$$

The Hamiltonian $\mathcal{H} = p q_t - L$ reads then:

$$\begin{aligned} \mathcal{H} = &\frac{c^4}{8\alpha^2} \Pi_\delta^2 + \frac{c^4}{2\delta^2} \Pi_\sigma^2 + c^3 \Pi_\sigma + \frac{\delta^2}{2} (\nabla \sigma)^2 \\ &+ 2\alpha^2 (\nabla \delta)^2 + 2\alpha f(\delta^2) + \frac{\delta^2\, c^2}{2} \end{aligned} \tag{43}$$

and the RGLE are given by (40) with $p = (\Pi_\delta, \Pi_\sigma)$ and q $= (\delta,\, \sigma)$. In particular, it is then easy to verify that the Galilean limit of these equations coincide with equation (16) in section (2.3) and that the static special relativistic solutions also minimize the free energy $\mathcal{F}$ introduced in section (2.1).

One can wonder what the special relativistic equivalent of the vortices introduced in section (2.3) are [16]. Let us say that a solution of the NLKGE is a vortex if there exists an inertial frame in which it is static and has cylindrical symmetry (with the density vanishing on the symmetry axis). Using (21), this definition automatically implies that a solution of the NLKGE is a vortex if, and only if, it is also a vortex for the NLSE. Let now r and θ be polar coordinates around the axis. The phase σ of a vortex solution is an integral multiple of $2\alpha\theta$ and the circulation I of the 4-gradient of σ around a closed space-like contour which 'surrounds' the vortex takes the form:

$$I = 4\pi\alpha\, q \tag{44}$$

where q is a positive or negative integer. Moreover, the enthalpy per particle H reads:

$$H = mc\left(1 - \left(\frac{r_{min}}{r}\right)^2\right)^{1/2} \tag{45}$$

where r_{min} is related to q and α by:

$$r_{min} = q\frac{2\alpha}{c} \tag{46}$$

This clearly shows that, in the special relativistic case, no hydrodynamical representation of the vortex is possible for r smaller than r_{min}. In particular, the special relativistic vortex cannot be interpreted as a line-like distribution of vorticity.

5 General relativistic self-gravitating fluids

This section is devoted to applications of the material developed in section 4 to self-gravitating fluids. This is achieved by extending the formalism to general relativity.

If the fluid is a Bose condensate of particles of rest-mass m, two characteristic length-scales can be defined: the Compton length $\hbar/mc$ and the gravitational radius $2Gm/c^2$. These two length-scales would be equal for a particle with a Planck mass $\sqrt{\hbar c/2G}$. At such scales, a quantum theory of gravity would be required for consistency.

For the temptative applications that we consider in this section, the quantum wave-length is much smaller than the gravitational radius and the theory presented here should be of some relevance.

5.1 Fundamentals

The correct action $\mathcal{A}_g$ describing the minimal coupling between the complex scalar field Φ and Einstein's gravitational field reads:

$$\mathcal{A}_g = \frac{1}{c}\int \sqrt{-g}\, d^4x \left(L - \frac{c^4}{16\pi G}R\right) \tag{47}$$

where G is Newton's gravitational constant, g stands for the determinant of the metric tensor and R for the scalar curvature of the metric-compatible connection. Variation of $\mathcal{A}_g$ with respect to Φ gives the curved space-time generalization of equation (21):

$$2\alpha^2 \nabla_\mu \nabla^\mu \Phi + 2\alpha \Phi f'(|\Phi|^2) + \frac{c^2}{2} \Phi = 0 \tag{48}$$

and the variation with respect to the metric furnishes Einstein equations [27]. One could also consider more general coupling between gravitation and the scalar field, as for example the so-called conform coupling [28]. This will not be done here.

5.2 Spherically symmetric 'soliton stars'

A first interesting application of the formalism just presented lies in the study of spherically symmetric solutions to the equations of motion. This has been done by various authors [14, 15] with a pure semi-classical field theory point of view, their principal aim being to describe yet unobserved astrophysical objects usually known as boson stars. In the light of section (4.1), it is rather clear that the structure of this type of stars and, more generally, of any star made out of a barotropic, possibly dispersive fluid (in potential motion), should admit a rather simple description in hydrodynamical language. As a matter of fact, it is possible [26] to derive for these stars an equivalent of the well-known Tollmann-Oppenheimer-Volkoff (TOV) equation. This derivation and the existing supplementary relations between the different unknown functions which are necessary to its solution are fully discussed in [16]. The standard Newtonian limit of the TOV-like system can be shown [16] to be a NLSE equation coupled to a gravitational potential obeying a Poisson equation with a source term $-4\pi\rho G$. This Newtonian self-gravitational system has been considered independently by S. Rica [29].

5.3 Homogeneous isotropic cosmological models

An interesting application of the relativistic formalism is the study of the equations governing the evolution of an isotropic 'toy-universe'. They are presented in [16], where it is shown that they give back, in suitable regimes, a standard Friedman-Robertson-Walker cosmology as well as Linde's chaotic inflation model.

6 Conclusion

The formalisms we have reviewed in this paper make it possible to deal with both Newtonian and Einsteinian perfect barotropic fluids with nonlinear wave equations.

In the case of simple Galilean free shear-flows, the numerical computations we have presented show the ability of NLSE to capture subtle hydrodynamical mechanisms such as vortex reconnection. Furthermore, in the case of superfluids modeled as weakly interacting Bose condensates, NLSE-type descriptions present the interest of naturally containing quantum vortices. This is an important advantage over the more conventional description of superflows in term of classical Euler equations supplemented with a quantification condition on the velocity circulation. As we have demonstrated, NLSE-type descriptions can be tuned to accommodate arbitrary equations of state and dispersion relations. It seems to us that they thus have a great potential for the quantitative explanation of phenomena in real superfluids such as Helium He II, provided that the temperature is low enough for the normal part of the flow to be neglected.

We have shown that the Galilean results can be quite simply extended to special relativity, thereby obtaining a natural description of relativistic barotropic fluids. Such a description is a necessary step to obtain a general relativistic consistent theory of a self-gravitating superfluid. The temptative results concerning self-gravitating bodies presented in section 5 show that this is perhaps the simplest way to introduce a non trivial fluid into general relativity. We are confident that careful studies of such toy models can shed new light on fundamental cosmological problems.

References

1. E. A. Spiegel. Fluid dynamical form of the linear and nonlinear schrödinger equations. *Physica D*, 1:236, 1980.
2. A. L. Fetter. Vortices in an imperfect bose gas iv. translational velocity. *Phys. Rev.*, 151:100, 1966.
3. J. C. Neu. Vortices in complex scalar fields. *Physica D*, 43:385, 1990.
4. F. Lund. Defect dynamics for the nonlinear schrödinger equation derived from a variational principle. *Phys.Rev.Lett.*, A 159:245, 1991.
5. R. J. Donnelly. *Quantized Vortices in Helium II.* Cambridge Univ. Press, 1991.
6. P. Nozières and D. Pines. *The Theory of Quantum Liquids.* Adv. Book Classics, Addison Wesley, 1990.
7. Y. Pomeau T. Frisch and S. Rica. Transition to dissipation in a model of superflow. *Phys.Rev.Lett.*, 69:1644, 1992.
8. Y. Pomeau and S. Rica. Model of superflow with rotons. *Phys. Rev. Lett.*, 71,2:247, 1993.
9. C. Nore, M. Brachet, and S. Fauve. Numerical study of hydrodynamics using the nonlinear schrödinger equation. *Physica D*, 65:154–162, 1993.
10. C. Nore, M. Abid, and M. Brachet. Simulation numérique d'écoulements cisaillés tridimensionnels à l'aide de l'équation de schrödinger non linéaire. *C.R.Acad.Sci. Paris*, 319 II(7):733, 1994.
11. J. Koplik and H. Levine. Vortex reconnection in superfluid helium. *Phys. Rev. Lett.*, 71:1375–1378, 1993.
12. C. Nore, M. Brachet, E. Cerda, and E. Tirapegui. Scattering of first sound by superfluid vortices. *Phys. Rev. Lett.*, 72(16):2593–2596, 1994.
13. J. C. Neu. Vortex dynamics of the nonlinear wave equation. *Physica D*, 43:407, 1990.
14. R. Friedberg, T.D. Lee, and Y. Pang. Mini-soliton stars. *Phys. Rev. D*, 35:3640, 1987.

15. N. Straumann. *Fermion and Boson stars in Relativistic Gravity Research.* Springer Verlag, Berlin, j. ehlers and g. schfer edition, 1992.
16. F. Debbasch and M. E. Brachet. Relativistic hydrodynamics of semiclassical quantum fluids. *to appear in Physica D*, 1995.
17. L. Landau and E. Lifchitz. *Fluid Mechanics*, volume 6. Pergamon Press, 1980.
18. T. Frisch, S. Rica, P. Coullet, and J. M. Gilli. Spiral waves in liquid crystal. *Phys. Rev. Lett.*, 72(10):1471, 1994.
19. D. Gottlieb and S. A. Orszag. *Numerical Analysis of Spectral Methods.* SIAM, Philadelphia, 1977.
20. M. P. Kawatra and R. K. Pathria. Quantized vortices in imperfect bose gas. *Phys.Rev.*, 151:1, 1966.
21. W. Eckhaus. *Studies in Nonlinear Stability Theory.* Springer, Berlin, 1965.
22. M. Abid and M. Brachet. Numerical characterisation of the dynamics of vortex f ilaments in round jets. *Phys. Fluids A*, 5(11):2582–2584, November 1993.
23. T. Kambe and T. Takao. Motion of distorted vortex rings. *J.Phys.Soc.Jap.*, 31(2):591–599, 1971.
24. G. K. Batchelor. Axial flow in trailing line vortices. *J. Fluid Mech.*, 20:645–658, 1964.
25. O. Cadot, S. Douady, and Y. Couder. Characterization of the low-pressure filaments in a three-dimensional turbulent shear flow. *Phys. Fluids*, 7(3):630, 1995.
26. F. Debbasch and M. E. Brachet. Nonlinear acoustics in a special relativistic superfluid. *submitted to Physica D*, 1995.
27. L. Landau and E. Lifchitz. *The Classical Theory of Fields*, volume 2. Pergamon Press, 1980.
28. R. Wald. *General Relativity.* Univ. of Chicago press, chicago edition, 1984.
29. S. Rica. *Défauts et Structures dans les Systèmes hors d'équilibre.* PhD thesis, Institut Non Linéaire de Nice, 1993.